

Fed-TDA: Federated Tabular Data Augmentation on Non-IID Data

Shaoming Duan¹², Chuanyi Liu^{123*}, Peiyi Han¹²³, Tianyu He¹², Yifeng Xu¹, Qiyuan Deng¹, Yuhao Zhang¹, Xinyu zha¹

¹School of Computer Science, Harbin Institute of Technology (Shenzhen), Shenzhen 518055, China

²Institute of Data Security, Harbin Institute of Technology (Shenzhen), Shenzhen 518055, China

³Department of New Networks, Peng Cheng Laboratory, Shenzhen 518000, China

Abstract

Non-independent and identically distributed (non-IID) data is a key challenge in federated learning (FL), which usually hampers the optimization convergence and the performance of FL. Existing data augmentation methods based on federated generative models or raw data sharing strategies still suffer from low performance, privacy protection concerns, and high communication overhead in decentralized tabular data. To tackle these challenges, we propose a federated tabular data augmentation (Fed-TDA) method that synthesizes fake tables using some low-dimensional statistics (e.g., distributions of each column and global covariance). Specifically, we propose the multimodal distribution transformation and inverse cumulative distribution mapping to synthesize continuous and discrete columns in tabular data according to the pre-learned statistics, respectively. Furthermore, we theoretically analyze that our Fed-TDA not only preserves data privacy but also maintains the distribution of the original data and the correlation between columns. Through extensive experiments on five real-world tabular datasets, we demonstrate the superiority of Fed-TDA over the state-of-the-art methods in test performance, statistical similarity, and communication efficiency. Code is available at <https://github.com/smduan/Fed-TDA.git>.

Introduction

In real-world applications, tabular data is the most common data type (Shwartz-Ziv and Armon 2022), which has been widely used in many relational database-based applications, such as medicine, finance, manufacturing, climate science, etc. Numerous organizations are using these data and machine learning (ML) to optimize their processes and performance. The wealth of data provides huge opportunities for ML applications. However, most of these tabular data are highly sensitive and typically distributed across different organizations. Due to privacy and regulatory concerns, these organizations are reluctant to share their private data.

In response to these concerns, federated learning (FL) (McMahan et al. 2017; Li et al. 2020a) has been extensively studied in recent years, where multiple participants jointly train a shared deep learning model under the coordination of a central server without transmitting their local data. Since

FL provides a feasible solution for data privacy, confidentiality, and data ownership, it has been applied in various tabular data applications, e.g., credit card detection (Duan et al. 2022), drug discovery (Chen et al. 2021), and traffic flow prediction (Qi et al. 2021). However, a key challenge for FL is that the data of different parties are non-independent and identically distributed (non-IID), which can seriously degrade the performance of FL (Li, He, and Song 2021; Li et al. 2022).

Existing studies for solving the non-IID problem can be roughly divided into two categories: *algorithm-based methods* and *data-based methods*. Algorithm-based methods mitigate the weight drift between clients and the server by designing appropriate loss functions (Li et al. 2020b; Li, He, and Song 2021) or personalized federated learning strategies (Zhu et al. 2021; Tan et al. 2022). However, both our experimental results and the studies in (Li et al. 2022) show that these methods do not always perform better than vanilla FedAvg (McMahan et al. 2017). Data-based methods perform data augmentation by sharing raw data (Yoon et al. 2021; Jeong et al. 2020; Oh et al. 2020) or generators (Wen et al. 2020; Augenstein et al. 2019; Wen et al. 2022), which convert non-IID data to IID data and fundamentally eliminate data distribution shifts. Compared with algorithm-based methods, numerous studies on image datasets show that data-based methods can effectively improve the performance of FL (Yoon et al. 2021; Luo et al. 2021; Wen et al. 2022).

Unfortunately, existing federated data augmentation methods directly applied to tabular data still suffer from the following challenges. Firstly, these methods fail to achieve high performance on tabular data. Unlike images, tabular data usually consists of a mixture of continuous and discrete columns. Synthesizing such mixed types of data remains a challenge for GAN-based methods, especially in terms of column distributions and correlations between columns (Xu et al. 2019; Lee et al. 2021). Furthermore, non-IID data will further degrade the performance of federated GANs (Zhao et al. 2021a). Secondly, since that tabular data usually contains sensitive information, sharing raw data or trained generators with other parties will compromise the privacy of the private data. Finally, exchanging raw data or generators between the server and clients will impose significant additional communication overhead.

*The corresponding author: liuchuanyi@hit.edu.cn.

To tackle these challenges, we propose Fed-TDA, a federated tabular data augmentation method for addressing the non-IID problem by synthesizing fake tables. The core idea of Fed-TDA is to synthesize tabular data with only some low-dimensional statistics (e.g., distributions of each column and global covariance). To maintain the distribution of the original data, we propose multimodal distribution transformation (MDT) and inverse cumulative distribution mapping (ICDM) to convert the random data following the standard normal distribution into continuous data following the multimodal distribution and discrete data following the cumulative distribution, respectively. In addition, to preserve the correlation between columns in the original data, our third innovation is to synthesize tabular data through a covariance-constrained data synthesis method based on global covariance, ICDM, and MDT. Unlike GAN-based methods, our Fed-TDA is a statistical model and will not be affected by non-IID data. In particular, we provide a theoretical analysis that our Fed-TDA not only protects data privacy but also preserves the distributions of the original data and the correlation between the columns.

Our main contributions can be summarized as follows:

- (1) We propose Fed-TDA, a federated data augmentation method for solving the non-IID problem in decentralized tabular data. To the best of our knowledge, this is the first attempt to study federated data augmentation on non-IID tabular data.
- (2) We propose a novel federated tabular data synthesis method for data augmentation based on some low-dimensional statistics. We theoretically provide a utility guarantee and privacy guarantee for our method.
- (3) We evaluate our Fed-TDA on five real-world datasets with various data distributions among participants. The experimental results show the superiority of our Fed-TDA in terms of test performance, statistical similarity, and communication efficiency.

Related Work and Background

Federated Learning with non-IID Data

In this paper, we focus on addressing the non-IID problem on decentralized tabular data. Existing relevant works can be roughly divided into two categories: algorithm-based methods and data-based methods.

Algorithm-based Methods. To mitigate the weight drift caused by the data distribution skew among clients, some robust loss functions are designed for FL. FedProx (Li et al. 2020b) adds a regularization term to the loss function to reduce the difference between the global and local models. SCAFFOLD (Karimireddy et al. 2020) performs control variates to correct for the weight drift in its local updates. MOON (Li, He, and Song 2021) utilizes contrastive loss to correct the training of local models. Unlike loss function-based methods, some personalized federated learning strategies are proposed to train personalized models for individual participants rather than a shared global model. In personalized federated learning, local fine-tuning (Tan et al. 2022), meta-learning (Fallah, Mokhtari, and Ozdaglar 2020; Yue

et al. 2022), multi-task learning (Marfoq et al. 2021; Sattler, Müller, and Samek 2020), and client clustering methods (Sattler, Müller, and Samek 2020; Ghosh et al. 2020) strategies are used to learn personalized models. However, as suggested in (Li et al. 2022), algorithm-based methods do not always perform better than vanilla FedAvg (McMahan et al. 2017).

Data-based Methods The key motivation of data-based methods is to convert non-IID data into IID by data augmentation strategies. Existing data augmentation methods can be divided into two categories: data sharing and data synthesis. Data sharing-based methods achieve data augmentation by directly sharing raw data (Jeong et al. 2020, 2018; Yoshida et al. 2020) or masked data (Yoon et al. 2021; Oh et al. 2020) which generated by mixup (Zhang et al. 2018) or XOR operation. Unlike data sharing methods, data synthesis methods synthesize fake data to eliminate distribution skew by sharing a trained generative model (Wen et al. 2020; Augenstein et al. 2019; Wen et al. 2022). Numerous studies have shown that data-based methods can effectively alleviate the non-IID problem on image data (Wen et al. 2022). However, these methods still suffer from privacy leakage and high communication overhead. In particular, data-based methods fail to achieve high performance on tabular data.

Differential Privacy

Definition 3.1. (Differential Privacy (Dwork and Roth 2014)) A randomized algorithm \mathcal{A} is (ϵ, δ) -differential privacy if for any output subset S and two neighboring datasets D and D' satisfies:

$$P(\mathcal{A}(D) \in S) \leq e^\epsilon \cdot P(\mathcal{A}(D') \in S) + \delta \quad (1)$$

where $\mathcal{A}(D)$ and $\mathcal{A}(D')$ are the output of the algorithm for neighboring datasets D and D' , respectively, and P is the randomness of the noise in the algorithm. The privacy budget ϵ is used to control the level of privacy. The smaller the ϵ , the better the privacy.

The Gaussian mechanism is a classical perturbation mechanism for (ϵ, δ) -differential privacy (Dwork and Roth 2014). For any deterministic vector-valued computation function $f: X \rightarrow R^d$, a Gaussian perturbation mechanism \mathcal{M} is obtained by computing the function f on the input data x and then adds random noise sampled from a Gaussian distribution to the output $\mathcal{M}(x) = f(x) + N(0, \sigma^2 I)$, where $N(0, \sigma^2 I)$ denotes a Gaussian distribution with a mean of 0 and a standard deviation of σ . For any function f have the global l_2 -sensitivity $\Delta = \max_{x, x'} \|f(x) - f(x')\|_2$, the

Gaussian mechanism \mathcal{M} with $\sigma \geq \frac{\Delta \cdot \sqrt{2 \ln(1.25/\delta)}}{\epsilon}$ is (ϵ, δ) -differential privacy (Dwork and Roth 2014).

Fed-TDA

Problem Formulation

In this paper, we follow the typical assumption of FL that all participants including the server are honest-but-curious. Suppose there are K clients in FL, and each client possesses

a local tabular dataset $X_k = (x_k, y_k), k = (1, 2, \dots, K)$, where x_k and y_k represent the features and labels of client k . The goal of FL is to learn a shared model θ over the decentralized dataset $X = \bigcup_{k \in [K]} X_k$. The objective of vanilla FedAvg (McMahan et al. 2017) is:

$$\arg \min_{\theta} \mathcal{L}(\theta) = \sum_{k=1}^K \frac{N_k}{N} \mathbb{E}_{(x,y) \sim X_k} [l_k(\theta, (x, y))] \quad (2)$$

where $\mathbb{E}_{(x,y) \sim X_k} [l_k(\theta, (x, y))]$ represents the empirical loss of client k , N_k denotes the number of samples in client k , $N = \sum_{k=1}^K N_k$ is the total number of samples over all clients. From a statistical perspective, the data of k -th client can be denoted as $P_x(x_k, y_k) = P_k(x_k|y_k)P_k(y_k)$, which represents the joint probability between x_k and y_k . Then, the joint distribution of global data is $P(x, y)$. In FL, we wish that the data distribution of each client is similar to the global data ($P_i(x_i, y_i) = P_j(x_j, y_j) = P(x, y), i \neq j$).

However, in real-world applications, the data is non-IID, $P_i(x_i, y_i) \neq P_j(x_j, y_j), i \neq j$, which will lead to weight drift and degrade the performance of FL. To solve this problem, we are committed to create an IID data ($P_i(x_i, y_i) \approx P_j(x_j, y_j) \approx P(x, y), i \neq j$) by data augmentation. The design goals of our method are as follows: (1) **High performance**. The data augmentation method needs to ensure the utility of the augmented tables in terms of data distributions and correlation between columns and further improve the performance of the FL; (2) **Privacy preserving**. The privacy of the raw data must be protected during the data augmentation processes. Specifically, the local training data cannot be shared with other clients or the server and the augmented data cannot reveal private information; (3) **Low communication costs**. The communication resources of FL are limited, and high additional communication overhead should not be introduced in the process of data augmentation; (4) **High flexibility and scalability**. Data augmentation should be independent of the FL model so that various FL algorithms can be flexibly adapted without any modification.

Federated Tabular Data Augmentation

Figure 1 shows an overview of Fed-TDA. Firstly, we compute the global multimodal distributions in continuous columns and the global frequency of categories in discrete columns from the decentralized tabular data. Secondly, we transform the tabular data into representations that follow the standard normal distribution by the proposed MDT and ICDM locally. After that, we compute the global covariance from the transformed data representations under the coordination of the server. Finally, each client synthesizes the fake data for data augmentation from a noise matrix following the standard multivariate normal distribution based on the pre-learned statistics, MDT, and ICDM. The detailed procedures of Fed-TDA are shown in Algorithm 1 and 2.

Multimodal Distribution Transformation Theoretically, continuous columns generally follow a multimodal distribution (Lindsay 1995), so any continuous column can be approximated by a finite number of Gaussian mixture distributions. In Fed-TDA, we design a multimodal distribution transformation to estimate a Mixture Gaussian Model

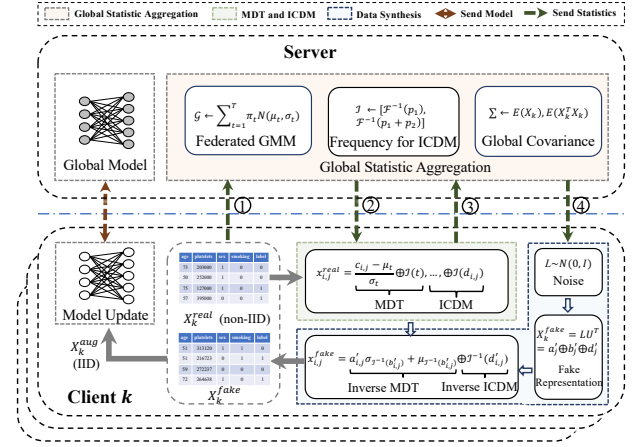


Figure 1: An overview of Fed-TDA. ① sends local statistics, including the parameters of federated GMM and the frequency of categories. ② returns the parameters of federated GMM and ICDM. ③ sends local expectations $E(X_k)$ and $E(X_k^T X_k)$. ④ returns the global covariance Σ .

Algorithm 1: Fed-TDA (Server Side)

Input: Global data set $X = (X_1, X_2, \dots, X_K)$, number of clients K , number of federated training rounds R .

Output: Well trained model θ .

- 1: $\mathcal{G} \leftarrow$ estimate the parameters (μ, σ, π) of Global GMM from each continuous column by the customized federated GMM
- 2: Compute the global frequency of categories in each discrete columns and construct the ICDM \mathcal{I}
- 3: **for** $k = 0, 1, \dots, K - 1$ **do**
- 4: Encode the local data by DMT and ICDM
- 5: Compute local expectation $E(X_k), E(X_k^T X_k)$
- 6: **end for**
- 7: Compute global covariance Σ by Equation (3).
- 8: $\Sigma = \Sigma + N(0, \sigma^2 I)$
- 9: Compute the Cholesky decomposition $\Sigma = UU^T$
- 10: **for** each client $k = 1, \dots, K$ in parallel **do**
- 11: $X_k' \leftarrow$ LocalDataSynthesis($\mathcal{G}, \mathcal{I}, U$)
- 12: **end for**
- 13: **for** each round $r = 1, \dots, R$ **do**
- 14: **for** each client $k = 1, \dots, K$ in parallel **do**
- 15: $\theta_k^{r+1} \leftarrow$ update local model θ^r using $(X_k' \cup X_k)$
- 16: **end for**
- 17: $\theta^{r+1} \leftarrow \sum_{k=1}^K \frac{N_k}{N} \theta_k^{r+1}$
- 18: **end for**
- 19: **return** θ^{r+1}

(GMM) for each continuous column and transform them into the representations that follow the standard normal distribution. Specifically, each value from the continuous column is represented as two scalars, one representing the normalized value and the other representing the Gaussian distribution it follows.

Firstly, we customize the variational Bayesian GMM al-

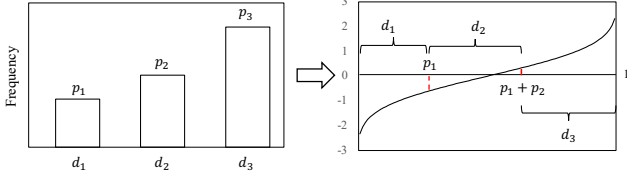


Figure 2: An example of ICDM. Categories are sorted by their frequency and then represented by a value randomly sampled from the corresponding inverse cumulative distribution of standard normal distribution.

Categorical	Cumulative Distribution	Inverse Cumulative Distribution
d_1	$[0 + \lambda, p_1]$	$[\mathcal{F}^{-1}(0 + \lambda), \mathcal{F}^{-1}(p_1)]$
d_2	$[p_1, p_1 + p_2]$	$[\mathcal{F}^{-1}(p_1), \mathcal{F}^{-1}(p_1 + p_2)]$
d_3	$[p_1 + p_2, 1 - \lambda]$	$[\mathcal{F}^{-1}(p_1 + p_2), \mathcal{F}^{-1}(1 - \lambda)]$

Table 1: Mapping of categories in Figure 2.

gorithm (Corduneanu and Bishop 2001) in FL to learn the global GMM for each continuous column C_i . The details of the designed federated VB-GMM algorithm are shown in Appendix A. From C_i , we learn a global GMM with T Gaussian distributions $P_{C_i}(c_{i,j}) = \sum_{t=1}^T \pi_t N(c_{i,j} | \mu_t, \sigma_t)$, where π_t represents the mixture weight of t -th Gaussian distribution. $N(c_{i,j} | \mu_t, \sigma_t)$ represents the t -th Gaussian distribution with mean μ_t and standard deviation σ_t . Then, each value $c_{i,j}$ in C_i is represented as $a_{i,j} \oplus b_{i,j}$, where $a_{i,j} = \frac{c_{i,j} - \mu_t}{\sigma_t}$, $b_{i,j} = t$, and \oplus represents the concatenate operation. Then, each row is represented as $x_j = a_{1,j} \oplus b_{1,j} \oplus \dots \oplus a_{n_c,j} \oplus d_{1,j} \oplus \dots \oplus d_{n_d,j}$, where $d_{i,j}$ represents the value of discrete column, n_c and n_d are the number of continuous and discrete columns, respectively. Note that, $b_{i,j}$ and $d_{i,j}$ represent discrete values.

Inverse Cumulative Distribution Mapping To model the discrete columns, we design the inverse cumulative distribution mapping to estimate the cumulative distribution for each discrete column and convert each category in the discrete columns into a continuous value that follows the standard normal distribution. Figure 2 shows an example of ICDM. Firstly, for each discrete column D_i , we compute the global frequency of each category $d_{i,j}$ from each client. For instance, in Figure 2, there are three categories, namely d_1 , d_2 and d_3 . The global frequencies of these three categories are p_1 , p_2 and p_3 , respectively. Then, each category is sorted by its frequency, such as $p_1 \leq p_2 \leq p_3$ in Figure 2. Finally, each category d_j in D_i is represented by a value randomly sampled from the corresponding interval of the inverse cumulative distribution of the standard normal distribution. Table 1 shows the inverse cumulative distribution mapping of example categories in Figure 2. As shown in Table 1, d_1 is represented as f_1 , where $f_1 \in [\mathcal{F}^{-1}(0 + \lambda), \mathcal{F}^{-1}(p_1)]$, $\mathcal{F}^{-1}(\cdot)$ represents the inverse cumulative distribution function of the standard normal distribution and λ is a small parameter mainly used to prevent the output of the \mathcal{F}^{-1} function from being $-\infty$ or $+\infty$. In this paper, we set the pa-

Algorithm 2: LocalDataSynthesis($\mathcal{G}, \mathcal{I}, U$)

Input: The parameters of global GMM \mathcal{G} , the parameter of ICDM \mathcal{I} , the unitary matrix U .

Output: Synthetic data X^s .

- 1: Randomly sample $L \sim N(0, I) \in \mathcal{R}^{N_s \times l}$
 - 2: $X' = LU^T = [x'_i]_{i=1}^{N_s} \in \mathcal{R}^{N_s \times l}$, where $x'_i = a'_{i,1} \oplus b'_{i,1} \oplus \dots \oplus a'_{i,n_c} \oplus b'_{i,n_c} \oplus d'_{i,1} \oplus \dots \oplus d'_{i,n_d}$
 - 3: **for** each discrete representation b'_j and d'_j **do**
 - 4: $b_j^s \leftarrow \mathcal{I}^{-1}(b'_j)$
 - 5: $d_j^s \leftarrow \mathcal{I}^{-1}(d'_j)$
 - 6: **end for**
 - 7: **for** each continuous representation a'_j **do**
 - 8: $t \leftarrow b_j^s$
 - 9: Get the parameters $\sigma_{j,t}, \mu_{j,t}$ of t -th Gaussian distribution from \mathcal{G}
 - 10: $a_j^s \leftarrow a_j \sigma_{j,t} + \mu_{j,t}$
 - 11: **end for**
 - 12: $X^s = [x_i^s]_{i=1}^{N_s} \in \mathcal{R}^{N_s \times (n_c + n_d)}$, where $x_i^s = a_{i,1}^s \oplus \dots \oplus a_{i,n_c}^s \oplus d_{i,1}^s \oplus \dots \oplus d_{i,n_d}^s$
 - 13: **return** X^s
-

parameter $\lambda = 10^{-4}$.

Global Covariance In addition to the distributions of each column, the synthetic data also needs to maintain the correlation between the columns in the original data. Therefore, we compute the global covariance Σ from the new representations. Let $N_k = |X_k|$ represent the number of samples in client k , the expectation of k -th client is $E(X_k) = \frac{1}{N_k} \sum_{j=1}^{N_k} x_{k,j} \in \mathcal{R}^{1 \times l}$, where l represents the dimension of features of the normalized representation and $l = 2n_c + n_d$. Then, each client send the local expectation $E(X_k)$ to the server and compute the global expectation $E(X) = \sum_{k=1}^K \frac{N_k}{N} E(X_k) \in \mathcal{R}^{1 \times l}$, where K is the number of clients. According to the formula of covariance that $\Sigma_X = E[(X - E(X))^T (X - E(X))]$, the global covariance is

$$\Sigma_X = \sum_{k=1}^K E(X_k^T X_k) - \left(\sum_{k=1}^K \frac{N_k}{N} E(X_k) \right)^T \left(\sum_{k=1}^K \frac{N_k}{N} E(X_k) \right) \quad (3)$$

where $X_k^T X_k = \sum_{j=1}^{N_k} x_{k,j}^T x_{k,j} \in \mathcal{R}^{l \times l}$. The detailed derivation of global expectation $E(X)$ and the global covariance Σ_X are provided in Appendix B.

Covariance-constrained Data Synthesis After obtaining the global covariance, each client synthesizes tabular data for data augmentation. Firstly, we inject the Gaussian noise into the global covariance $\Sigma_X = \Sigma_X + N(0, \sigma^2 I)$ and compute its Cholesky decomposition $\Sigma_X = UU^T, U \in \mathcal{R}^{l \times l}$ on the server (lines 8-9 in Algorithm 1). Then, the unitary matrix U is shared to each client.

Secondly, as shown in Algorithm 2, we sample a noise $L \sim N(0, I) \in \mathcal{R}^{N_s \times l}$ and compute the fake representation by $X' = LU^T = [x'_i]_{i=1}^{N_s} \in \mathcal{R}^{N_s \times l}$, where N_s represents the number of synthetic data. For each row $x'_i =$

Datasets	β	FedAvg	FedProx	Fedmix	DP-FedAvg-GAN	Fed-TGAN	Fed-TDA + FedAvg	Fed-TDA + FedProx
Clinical	$\beta = 0.05$	0.605±0.032	0.620±0.037	0.635±0.043	0.713±0.023	0.897±0.038	0.983±0.004	0.947±0.018
	$\beta = 0.1$	0.653±0.012	0.661±0.020	0.634±0.018	0.831±0.018	0.913±0.008	0.984±0.003	0.941±0.015
	$\beta = 0.5$	0.773±0.013	0.764±0.025	0.739±0.020	0.85±0.030	0.894±0.009	0.986±0.003	0.966±0.009
	$\beta = 100$ (IID)	0.975±0.007	-	-	-	-	-	-
Tuberculosis	$\beta = 0.05$	0.803±0.016	0.806±0.031	0.797±0.040	0.876±0.005	0.865±0.014	0.931±0.002	0.939±0.004
	$\beta = 0.1$	0.867±0.011	0.881±0.007	0.877±0.007	0.928±0.007	0.931±0.004	0.933±0.006	0.939±0.001
	$\beta = 0.5$	0.951±0.004	0.947±0.001	0.949±0.003	0.905±0.264	0.956±0.002	0.946±0.003	0.961±0.000
	$\beta = 100$ (IID)	0.976±0.002	-	-	-	-	-	-

Table 2: ROCAUC scores of different methods on Clinical and Tuberculosis datasets. The parameter of Dirichlet distribution β varies from 0.05 to 0.5, $K = 5$, privacy budget $\epsilon = \infty$, and the local epoch is 3.

Datasets	β	FedAvg	FedProx	Fedmix	DP-FedAvg-GAN	Fed-TGAN	Fed-TDA + FedAvg	Fed-TDA + FedProx
CovType	$\beta = 0.01$	0.364±0	0.484±0.016	0.364±0.000	0.485±0.004	0.367±0.002	0.529±0.019	0.612±0.007
	$\beta = 0.05$	0.364±0	0.358±0.009	0.607±0.003	0.487±0.000	0.366±0.002	0.589±0.006	0.620±0.002
	$\beta = 0.1$	0.491±0.006	0.512±0.037	0.492±0.008	0.570±0.005	0.488±0.016	0.600±0.003	0.620±0.003
	$\beta = 100$ (IID)	0.649±0.008	-	-	-	-	-	-
Intrusion	$\beta = 0.01$	0.590±0.125	0.856±0.050	0.575±0.074	0.900±0.048	0.783±0.004	0.956±0.008	0.950±0.012
	$\beta = 0.05$	0.762±0.008	0.970±0.005	0.765±0.011	0.967±0.009	0.826±0.046	0.970±0.004	0.983±0.004
	$\beta = 0.1$	0.978±0.005	0.987±0.000	0.975±0.015	0.986±0.002	0.988±0.000	0.980±0.002	0.985±0.000
	$\beta = 100$ (IID)	0.989±0.000	-	-	-	-	-	-
Body	$\beta = 0.01$	0.271±0.007	0.297±0.014	0.272±0.007	0.252±0.003	0.335±0.051	0.633±0.005	0.605±0.016
	$\beta = 0.05$	0.308±0.015	0.291±0.031	0.272±0.019	0.330±0.018	0.411±0.021	0.614±0.011	0.594±0.021
	$\beta = 0.1$	0.459±0.000	0.457±0.003	0.455±0.001	0.459±0.007	0.454±0.001	0.613±0.011	0.605±0.009
	$\beta = 100$ (IID)	0.734±0.006	-	-	-	-	-	-

Table 3: Test accuracy of different methods on CovType, Intrusion and Body datasets. The parameter of Dirichlet distribution β varies from 0.01 to 0.1, $K = 5$, privacy budget $\epsilon = \infty$, and the local epoch is 3.

$a'_{i,1} \oplus b'_{i,1} \oplus \dots \oplus a'_{i,n_c} \oplus b'_{i,n_c} \oplus d'_{i,1} \oplus \dots \oplus d'_{i,n_d}$ in X' , we first recover the discrete columns by ICDM. For instance, for each discrete representation $b'_{i,j}$ or $d'_{i,j}$, if $b'_{i,j}$ or $d'_{i,j} \in [\mathcal{F}^{-1}(0 + \lambda), \mathcal{F}^{-1}(p_1)]$, then $b^s_{i,j} \leftarrow d_1$ or $d^s_{i,j} \leftarrow d_1$. Then, the continuous columns are recovered by the inverse operation of MDT, $a^s_{i,j} = a'_{i,j} \sigma_{j,t} + \mu_{j,t}$, where $t = b^s_{i,j}$, $\mu_{j,t}$ and $\sigma_{j,t}$ represent the mean and the standard deviation of t -th Gaussian distribution, respectively. Finally, the synthetic data is represented as $X^s = [x^s_i]_{i=1}^{N_s} \in \mathcal{R}^{N_s \times (n_c + n_d)}$, where $x^s_i = a^s_{i,1} \oplus \dots \oplus a^s_{i,n_c} \oplus d^s_{i,1} \oplus \dots \oplus d^s_{i,n_d}$.

Utility of Synthetic Data

We ensure the utility of synthetic data from the perspective of data distribution and correlation between columns. Firstly, in Fed-TDA, the continuous and discrete columns are synthesized by MDT and ICDM, respectively. The proposed MDT and ICDM ensure that continuous and discrete columns in the synthetic data maintain the same multimodal and cumulative distributions as the original data, respectively. Secondly, Theorem 1 guarantees that the correlations between columns in the synthetic data are consistent with the original data. The detailed proof of Theorem 1 are given in Appendix C.

Theorem 1. $X \sim N(0, I)$, $X \in \mathcal{R}^{N \times l}$, the covariance of X is Σ_X and its Cholesky decomposition is $\Sigma_X = UU^T$. For $\forall L \sim N(0, I)$, $L \in \mathcal{R}^{N \times l}$. $Y = LU^T \in \mathcal{R}^{N \times l}$, we

have $\Sigma_Y = \Sigma_X$.

Privacy Analysis

Firstly, Fed-TDA strictly follows the standard FL framework (McMahan et al. 2017) and protects privacy at the basic level as each client only uploads some statistics rather than the raw data. Secondly, in the data synthesis phase, the differential privacy (DP) (Dwork and Roth 2014) is introduced to the shared covariance. As shown in Algorithm 2, the synthetic data is first constrained by global covariance. In addition, the post-processing property of DP (Dwork and Roth 2014) shows that any mapping of differential private output also satisfies the same-level DP. Thus, we inject Gaussian noise into the global covariance $\Sigma = \Sigma + N(0, \sigma^2 I)$, where $N(0, \sigma^2 I)$ represents the Gaussian distribution with mean 0 and standard deviation σ . To satisfy (ϵ, δ) -differential privacy, following (Dwork and Roth 2014), we set $\sigma = \frac{\Delta_\Sigma \sqrt{2 \ln(1.25/\delta)}}{\epsilon}$. Since the values of $\Sigma \in [-1, 1]$, then the l_2 -sensitivity of Σ is $\Delta_\Sigma = 2$ in this paper. We give the privacy guarantee of our Fed-TDA as follows.

Theorem 2. Fed-TDA is (ϵ, δ) -differential privacy. The proof of Theorem 2 follows the standard analysis of Gaussian mechanism in (Bassily 2019).

Experiments

Experimental Setup

Datasets We evaluate our Fed-TDA on five real-world tabular datasets, targeting binary and multi-class classification. The list of datasets is as follows: (1) **Clinical** (Chicco and Jurman 2020) is a dataset about Cardiovascular diseases (CVDs) that predicts mortality from heart failure information; (2) **Tuberculosis** (Warnat-Herresthal et al. 2021) is an RNA-seq dataset based on whole blood transcriptomes, which is used to predict tuberculosis from genetic information; (3) **CovType** (Blackard and Dean 1999) is for forest cover types prediction; (4) **Intrusion** is collected from the kddcup99 (Tavallaee et al. 2009) dataset and contains the top 10 types of network intrusions; (5) **Body** (Kaggle 2022) dataset comes from Kaggle and is provided by Korea Sports Promotion Foundation for predicting body performance. Clinical and Tuberculosis datasets are for binary classification, and CovType, Intrusion, and Body datasets are for multi-class classification.

To simulate the non-IID data, we follow the label skew method in (Li et al. 2022), where each client is allocated a proportion of the samples of each label according to the Dirichlet distribution. Specifically, we allocate a $p_{k,l}$ ($p_{k,l} \sim \text{Dir}(\beta)$) proportion of the samples of label l to participant k , where $\text{Dir}(\beta)$ represents the Dirichlet distribution with a parameter β ($\beta > 0$). Then, we can flexibly control the degree of the non-IID by varying the parameter β . The smaller the β is, the higher the degree of label distribution drift. More details on the presentation, statistics, and partitioning of the datasets are given in Appendix E.

Baseline Methods We compare our Fed-TDA with five state-of-art methods: one traditional FL method, **FedAvg** (McMahan et al. 2017); one algorithm-based method, **FedProx** (Li et al. 2020b); one data sharing-based method, **Fedmix** (Yoon et al. 2021); and two GAN-based methods, **DP-FedAvg-GAN** (Augenstein et al. 2019) and **Fed-TGAN** (Zhao et al. 2021a). Besides FedAvg (**Fed-TDA + FedAvg**), we also extended our Fed-TDA to Fedprox (**Fed-TDA+FedProx**). For the classifier, we adopt a simple deep learning model with fully-connected layers for the tabular data. The metric of the binary classification task is ROCAUC, and the multi-class classification task is accuracy. More implementation details are given in Appendix E.

Performance on Non-IID Federated Learning

Varying Non-IID Settings Table 2 and Table 3 show the test performance ($mean \pm std$) of binary and multi-class classification tasks under the different non-IID settings, respectively. In almost all cases, our Fed-TDA achieves the best performance. In addition, the test performance of other methods increases as β increases, while Fed-TDA is always stable and close to IID data. This shows that our Fed-TDA can effectively eliminate the non-IID problem by synthesizing high-quality data for data augmentation. For GAN-based methods and Fedmix, most of them perform well in some cases compared with FedAvg. However, there is still a performance gap compared with Fed-TDA because they are

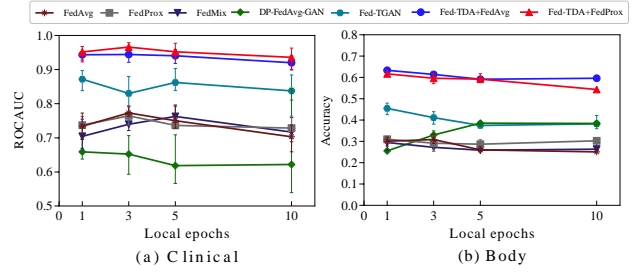


Figure 3: Test performance under varying number of local epochs on the Clinical and Body datasets. Where $\beta = 0.05$ and $K = 5$.

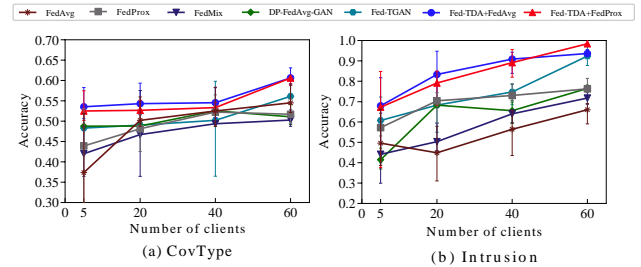


Figure 4: Test performance under varying number of clients on the CovType and Intrusion datasets. We set $\beta = 0.05$, the local epoch is 3, and the number of samples per client is kept constant. K varies from 5 to 60.

limited in the quality of synthetic tabular data under non-IID data. For FedProx, it performs similarly to FedAvg because it does not fundamentally eliminate the distribution shift problem, which is consistent with the conclusion in (Li et al. 2022).

Varying Local Epochs We study the impact of the number of local epochs on test performance. Figure 3 shows the test performance (ROCAUC or accuracy) of baseline methods on the Clinical and Body datasets (5 times per case). As the number of local epochs increases from 1 to 10, Fed-TDA achieves the best and most robust performance. It shows the robustness of our Fed-TDA to local training parameters. More results on other datasets are given in Appendix F.

Varying Local Clients Figure 4 investigates the impact of the number of clients on test performance on the CovType and Intrusion datasets (5 times per case). Each client kept a fixed number of samples. As the number of clients increases from 5 to 60, the test performance of all methods improves. This is because the amount of data and features will increase with the number of clients. In almost all cases, we observe the superior performance of Fed-TDA compared to other baseline methods.

Learning Curves Figure 5 shows the learning curves on the CovType and Body datasets. As shown in Figure 5, Fed-TDA achieves the fastest convergence and the best performance in the non-IID scenario. This is because the proposed Fed-TDA converts non-IID data to IID data by pro-

Methods	Clinical						Intrusion					
	$\beta = 0.05$		$\beta = 0.1$		$\beta = 0.5$		$\beta = 0.01$		$\beta = 0.05$		$\beta = 0.1$	
	JSD	WD	JSD	WD	JSD	WD	JSD	WD	JSD	WD	JSD	WD
DP-FedAvg-GAN	0.422	0.308	0.303	0.317	0.345	0.318	0.588	0.259	0.510	0.312	0.618	0.232
Fed-TGAN	0.165	0.095	0.164	0.102	0.132	0.128	0.278	0.279	0.211	0.264	0.181	0.254
Fed-TDA	0.082	0.091	0.081	0.081	0.086	0.095	0.064	0.093	0.064	0.093	0.064	0.093

Table 4: The statistical similarity for DP-FedAvg-GAN, Fed-TGAN, and Fed-TDA. Where $K = 5$.

Datasets	FedAvg/FedProx		Fedmix		DP-FedAvg-GAN		Fed-TGAN		Fed-TDA	
	U	D	U	D	U	D	U	D	U	D
Clinical	367.18	367.18	0.0039	0.0156	178.45	188.82	662	662	0.4358	0.4402
Tuberculosis	18052	18052	18.21	72.84	70971	71179.93	233000	233000	6274.3	6284.6
CovType	436.55	436.55	3.3525	13.4103	342.51	353.8	1510	1510	0.6951	0.7034
Intrusion	450.59	450.59	8.0300	32.1200	291.73	302.74	2290	2290	2.4446	2.4665
Body	354.15	354.15	0.2292	0.9168	174.54	184.89	1010	1010	0.6204	0.6263

Table 5: The total communication costs (MB) of federated learning. "U" and "D" are short for "Upload" and "Download", respectively. Where $\beta = 0.05$ and $K = 5$.

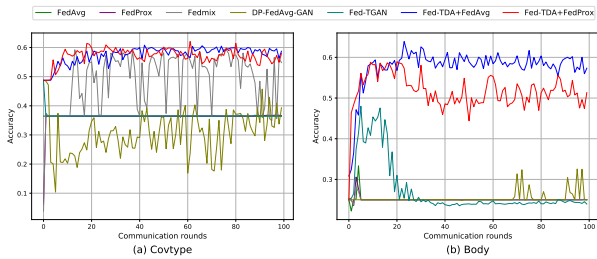


Figure 5: Learning curves of the baseline methods on the CovType and Body datasets. Where $\beta = 0.05$, $K = 5$, the local epoch is 3.

viding high-quality synthetic data. In contrast, the baseline methods do not converge or converge to a poor state. This indicates that the baseline methods cannot train a usable model.

Privacy Study

Figure 9 demonstrates the trade-off between the test performance of Fed-TDA and the privacy level on the Intrusion and CovType datasets. As shown in Figure 9, the test performance of our Fed-TDA improves as ϵ varies from 1 to ∞ . This is because the smaller ϵ is, the better the privacy but the lower the data utility. As ϵ increases from 1 to ∞ , the test accuracy of Fed-TDA increases from 0.908 to 0.97 on the Intrusion dataset, and from 0.517 to 0.589 on the CovType dataset. More results on other datasets are shown in Appendix F.

Statistical Similarity

Following (Zhao et al. 2021b), we use the average Jensen-Shannon Divergence (JSD) and the average Wasserstein Distance (WD) to quantitatively measure the statistical similar-

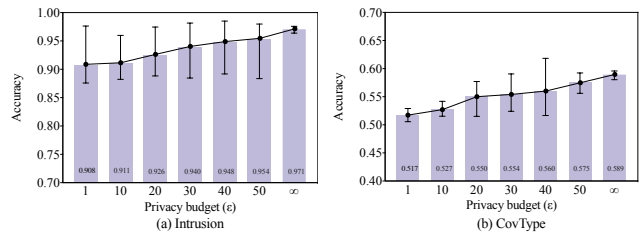


Figure 6: Trade-off between the test performance and the privacy level on the Intrusion and CovType datasets. Where $\beta = 0.05$, $K = 5$, the local epoch is 3, privacy budget $\delta = 10^{-4}$ and ϵ varies from 1 to ∞ .

ity between the synthetic and real data. The average JSD and average WD are used to measure discrete and continuous columns, respectively. Table 9 shows the statistical similarity results on the Clinical and Intrusion datasets. Compared with GAN-based methods, Fed-TDA consistently achieves the best similarity scores because the synthetic data generated by Fed-TDA keep the same statistical distribution as the real data as discussed in Section . In addition, as the β increases, the statistical similarity scores of GAN-based methods also get better. This shows that GAN-based methods are affected by Non-IID data. Unlike GAN-based methods, our Fed-TDA is a statistical model and will not be affected by non-IID data. More results on other datasets are given in appendix F.

Communication Costs

Table 5 shows the total communication costs for 100 communication rounds of federated training. In practice, the communication rounds of DP-FedAvg-GAN, Fed-TGAN, and Federated VB-GMM are 100, while Fedmix only exchanges once before training. Compared with the algorithm-

based method (FedProx) and GAN-based methods (DP-FedAvg-GAN and Fed-TGAN), the communication overhead of Fed-TDA is negligible. This is because they transmit the parameters of models or GANs iteratively, whereas Fed-TDA only exchanges low-dimensional statistics. Compared with Fedmix, Fed-TDA consumes less communication overhead on Covtype, Intrusion, and Body datasets, but more on others. Especially on the Tuberculosis dataset, the communication overhead of Fed-TDA far exceeds that of Fedmix. As analyzed in Appendix D, the communication costs of Fed-TDA is $O(n_c^2 + n_d^2)$. The Tuberculosis dataset contains 1240 samples but 18136 continuous columns, which makes Fed-TDA consume far more communication overhead than Fedmix. Therefore, a limitation of Fed-TDA is that it will incur a lot of additional communication overhead on high-dimensional data.

Conclusion

In this paper, we presented Fed-TDA, a federated tabular data augmentation method for solving the non-IID problem in federated learning. Unlike GAN-based methods, Fed-TDA synthesizes tabular data only using some simple statistics, including distributions of each column and global covariance. In Fed-TDA, the MDT and the ICDM are proposed to synthesize continuous columns and discrete columns, respectively. The effectiveness, privacy, and communication efficiency of Fed-TDA have been demonstrated from both theoretical and experimental perspectives.

References

- Augenstein, S.; McMahan, H. B.; Ramage, D.; Ramaswamy, S.; Kairouz, P.; Chen, M.; Mathews, R.; and y Arcas, B. A. 2019. Generative Models for Effective ML on Private, Decentralized Datasets. In *International Conference on Learning Representations*.
- Bassily, R. 2019. Linear queries estimation with local differential privacy. In *The 22nd International Conference on Artificial Intelligence and Statistics*, 721–729. PMLR.
- Blackard, J. A.; and Dean, D. J. 1999. Comparative accuracies of artificial neural networks and discriminant analysis in predicting forest cover types from cartographic variables. *Computers and electronics in agriculture*, 24(3): 131–151.
- Chen, S.; Xue, D.; Chuai, G.; Yang, Q.; and Liu, Q. 2021. FL-QSAR: a federated learning-based QSAR prototype for collaborative drug discovery. *Bioinformatics*, 36(22-23): 5492–5498.
- Chicco, D.; and Jurman, G. 2020. Machine learning can predict survival of patients with heart failure from serum creatinine and ejection fraction alone. *BMC medical informatics and decision making*, 20(1): 1–16.
- Corduneanu, A.; and Bishop, C. M. 2001. Variational Bayesian model selection for mixture distributions. In *Artificial intelligence and Statistics*, volume 2001, 27–34. Morgan Kaufmann Waltham, MA.
- Duan, S.; Liu, C.; Cao, Z.; Jin, X.; and Han, P. 2022. Fed-DR-Filter: Using global data representation to reduce the impact of noisy labels on the performance of federated learning. *Future Generation Computer Systems*, 137: 336–348.
- Dwork, C.; and Roth, A. 2014. The Algorithmic Foundations of Differential Privacy: Foundations and Trends in Theoretical Computer Science. *Hanover, MA: NOW Publishers*.
- Fallah, A.; Mokhtari, A.; and Ozdaglar, A. 2020. Personalized federated learning with theoretical guarantees: A model-agnostic meta-learning approach. *Advances in Neural Information Processing Systems*, 33: 3557–3568.
- Ghosh, A.; Chung, J.; Yin, D.; and Ramchandran, K. 2020. An efficient framework for clustered federated learning. *Advances in Neural Information Processing Systems*, 33: 19586–19597.
- Jeong, E.; Oh, S.; Kim, H.; Park, J.; Bennis, M.; and Kim, S.-L. 2018. Communication-efficient on-device machine learning: Federated distillation and augmentation under non-iid private data. *arXiv preprint arXiv:1811.11479*.
- Jeong, E.; Oh, S.; Park, J.; Kim, H.; Bennis, M.; and Kim, S.-L. 2020. Hiding in the crowd: Federated data augmentation for on-device learning. *IEEE Intelligent Systems*, 36(5): 80–87.
- Kaggle. 2022. Body performance data. <https://www.kaggle.com/datasets/kukuroo3/body-performance-data>.
- Karimireddy, S. P.; Kale, S.; Mohri, M.; Reddi, S.; Stich, S.; and Suresh, A. T. 2020. Scaffold: Stochastic controlled averaging for federated learning. In *International Conference on Machine Learning*, 5132–5143. PMLR.
- Lee, J.; Hyeong, J.; Jeon, J.; Park, N.; and Cho, J. 2021. Invertible Tabular GANs: Killing Two Birds with One Stone for Tabular Data Synthesis. *Advances in Neural Information Processing Systems*, 34: 4263–4273.
- Li, Q.; Diao, Y.; Chen, Q.; and He, B. 2022. Federated learning on non-iid data silos: An experimental study. In *2022 IEEE 38th International Conference on Data Engineering (ICDE)*, 965–978. IEEE.
- Li, Q.; He, B.; and Song, D. 2021. Model-contrastive federated learning. In *Proceedings of the IEEE/CVF Conference on Computer Vision and Pattern Recognition*, 10713–10722.
- Li, T.; Sahu, A. K.; Talwalkar, A.; and Smith, V. 2020a. Federated learning: Challenges, methods, and future directions. *IEEE Signal Processing Magazine*, 37(3): 50–60.
- Li, T.; Sahu, A. K.; Zaheer, M.; Sanjabi, M.; Talwalkar, A.; and Smith, V. 2020b. Federated optimization in heterogeneous networks. *Proceedings of Machine Learning and Systems*, 2: 429–450.
- Lindsay, B. G. 1995. Mixture models: theory, geometry, and applications. Ims.
- Luo, M.; Chen, F.; Hu, D.; Zhang, Y.; Liang, J.; and Feng, J. 2021. No fear of heterogeneity: Classifier calibration for federated learning with non-iid data. *Advances in Neural Information Processing Systems*, 34: 5972–5984.
- Marfoq, O.; Neglia, G.; Bellet, A.; Kamani, L.; and Vidal, R. 2021. Federated multi-task learning under a mixture of

- distributions. *Advances in Neural Information Processing Systems*, 34: 15434–15447.
- McMahan, B.; Moore, E.; Ramage, D.; Hampson, S.; and y Arcas, B. A. 2017. Communication-efficient learning of deep networks from decentralized data. In *Artificial intelligence and statistics*, 1273–1282. PMLR.
- Oh, S.; Park, J.; Jeong, E.; Kim, H.; Bennis, M.; and Kim, S.-L. 2020. Mix2FLD: Downlink federated learning after uplink federated distillation with two-way mixup. *IEEE Communications Letters*, 24(10): 2211–2215.
- Qi, Y.; Hossain, M. S.; Nie, J.; and Li, X. 2021. Privacy-preserving blockchain-based federated learning for traffic flow prediction. *Future Generation Computer Systems*, 117: 328–337.
- Sattler, F.; Müller, K.-R.; and Samek, W. 2020. Clustered federated learning: Model-agnostic distributed multitask optimization under privacy constraints. *IEEE transactions on neural networks and learning systems*, 32(8): 3710–3722.
- Shwartz-Ziv, R.; and Armon, A. 2022. Tabular data: Deep learning is not all you need. *Information Fusion*, 81: 84–90.
- Tan, A. Z.; Yu, H.; Cui, L.; and Yang, Q. 2022. Towards personalized federated learning. *IEEE Transactions on Neural Networks and Learning Systems*.
- Tavallaee, M.; Bagheri, E.; Lu, W.; and Ghorbani, A. A. 2009. A detailed analysis of the KDD CUP 99 data set. In *2009 IEEE symposium on computational intelligence for security and defense applications*, 1–6. Ieee.
- Warnat-Herresthal, S.; Schultze, H.; Shastry, K. L.; Manamohan, S.; Mukherjee, S.; Garg, V.; Sarveswara, R.; Händler, K.; Pickkers, P.; Aziz, N. A.; et al. 2021. Swarm learning for decentralized and confidential clinical machine learning. *Nature*, 594(7862): 265–270.
- Wen, H.; Wu, Y.; Li, J.; and Duan, H. 2022. Communication-Efficient Federated Data Augmentation on Non-IID Data. In *Proceedings of the IEEE/CVF Conference on Computer Vision and Pattern Recognition*, 3377–3386.
- Wen, H.; Wu, Y.; Yang, C.; Duan, H.; and Yu, S. 2020. A unified federated learning framework for wireless communications: Towards privacy, efficiency, and security. In *IEEE INFOCOM 2020-IEEE Conference on Computer Communications Workshops (INFOCOM WKSHPS)*, 653–658. IEEE.
- Xu, L.; Skoularidou, M.; Cuesta-Infante, A.; and Veeramachaneni, K. 2019. Modeling tabular data using conditional gan. *Advances in Neural Information Processing Systems*, 32.
- Yoon, T.; Shin, S.; Hwang, S. J.; and Yang, E. 2021. FedMix: Approximation of Mixup under Mean Augmented Federated Learning. In *International Conference on Learning Representations*.
- Yoshida, N.; Nishio, T.; Morikura, M.; Yamamoto, K.; and Yonetani, R. 2020. Hybrid-FL for wireless networks: Cooperative learning mechanism using non-IID data. In *ICC 2020-2020 IEEE International Conference on Communications (ICC)*, 1–7. IEEE.
- Yue, S.; Ren, J.; Xin, J.; Zhang, D.; Zhang, Y.; and Zhuang, W. 2022. Efficient federated meta-learning over multi-access wireless networks. *IEEE Journal on Selected Areas in Communications*, 40(5): 1556–1570.
- Zhang, H.; Cisse, M.; Dauphin, Y. N.; and Lopez-Paz, D. 2018. mixup: Beyond Empirical Risk Minimization. In *International Conference on Learning Representations*.
- Zhao, Z.; Birke, R.; Kunar, A.; and Chen, L. Y. 2021a. Fed-TGAN: Federated learning framework for synthesizing tabular data. *arXiv preprint arXiv:2108.07927*.
- Zhao, Z.; Kunar, A.; Birke, R.; and Chen, L. Y. 2021b. Ctabgan: Effective table data synthesizing. In *Asian Conference on Machine Learning*, 97–112. PMLR.
- Zhu, H.; Xu, J.; Liu, S.; and Jin, Y. 2021. Federated learning on non-IID data: A survey. *Neurocomputing*, 465: 371–390.

Appendix

A Federated VB-GMM

Gaussian Mixture Model (GMM) (Corduneanu and Bishop 2001) is a probabilistic model as shown in Equation (4).

$$p(x|\pi, \mu, \Sigma) = \sum_{t=1}^T \pi_t N(x|\mu_t, \Sigma_t) \quad (4)$$

where π_t is called mixing coefficients, represents the mixture weight of t -th Gaussian distribution. $N(x|\mu_t, \Sigma_t)$ represents t -th Gaussian distribution with mean μ_t and variance Σ_t . GMM is expressed as the sum of the number of K Gaussian distributions multiplied by the corresponding weight π_t . There are four parameters π, μ, Σ and K to be optimized when GMM is applied to a dataset.

Variational Bayesian Gaussian Mixture Model (VB-GMM) (Corduneanu and Bishop 2001) is a model which applying Variational Bayesian method to estimate the parameters of GMM. It introduces three distributions, Dirichlet, Gaussian, and Wishart as the prior distributions for π, μ , and Λ (inverse matrix of Σ), as shown in Equations (5), (6), (7) respectively.

$$\pi \sim Dir(\alpha) \quad (5)$$

$$\mu \sim N(m, (\beta\Lambda)^{-1}) \quad (6)$$

$$\mathcal{W}(W, \nu) \quad (7)$$

where α is a parameter of the Dirichlet distribution, which represents the prior distribution of π , m and β are parameters of the Gaussian distribution, which represent the prior distribution of μ , W , and ν are parameters of the Wishart distribution which represent the prior distribution of Λ . The parameters of GMM can be calculated by introducing the prior distribution of each parameter combined with the Variational EM algorithm (Corduneanu and Bishop 2001).

In this paper, we customize the variational Bayesian GMM algorithm (Corduneanu and Bishop 2001) under federated learning to learn the global GMM for each continuous column in decentralized tabular data $X = \{x_1, \dots, x_n\}$. The procedures of federated VB-GMM are as follows:

Step 1 (Initialization): Server

- Initialize $\alpha, m, \beta, \Lambda, W, \nu, T$ randomly, where α is a parameter of Dirichlet distribution of which is a prior distribution of π ($\pi \sim Dir(\alpha)$), m and β are parameters of a Gaussian distribution which is a prior distribution of μ ($\mu \sim N(m, (\beta\Lambda)^{-1})$), W and ν are parameters of a Wishart distribution which is a prior distribution of an inverse matrix Λ ($\Lambda \sim \mathcal{W}(W, \nu)$).
- Send $\alpha, m, \beta, \Lambda, W, \nu, T$ to each Client.

Step 2 (Variational E step): Client

- Each client get $\alpha, m, \beta, \Lambda, W, \nu, T$
- Update the precision Λ

$$\ln \tilde{\Lambda} = \sum_{d=1}^D \psi\left(\frac{\nu_t + 1 + d}{2}\right) + D \ln 2 + \ln |W_k| \quad (8)$$

- Compute the local responsibilities r_{nt}

$$\ln \tilde{\pi} = \psi(\alpha_t) - \psi\left(\sum_{i=1}^T (\alpha_i)\right) \quad (9)$$

$$r_{nt} = \pi_t |\Lambda_t|^{1/2} \times \exp\left\{-\frac{D}{2\beta_t} - \frac{\nu_t}{2}(x_n - m_t)^T W_t (x_n - m_t)\right\} \quad (10)$$

- Compute the mean \tilde{x}'_t of local data which belongs to the t -th mode

$$\tilde{x}'_t = \sum_{n=1}^{N_{client}} r_{nt} x_n \quad (11)$$

- Send $HE(r_{nt})$ and $HE(\tilde{x}'_t)$ to the server // $HE(\cdot)$ represents homomorphic encryption.

Step 3 (Variational E step): Server

- Get $HE(r_{nt})$ and $HE(\tilde{x}'_t)$ from each client
- Compute the global responsibilities N_t

$$HE(N_t) = \sum_{c \in C} HE(r_{nt}) \quad (12)$$

- Update the global mean \tilde{x}_t of the global data which belongs to the t -th mode

$$HE(\tilde{x}_t) = \frac{1}{N_t} \sum_{c \in C} HE(\tilde{x}'_t) \quad (13)$$

- Send $HE(N_t)$ and $HE(\tilde{x}_t)$ to each client

Step 4 (Variational M step): Client

- Each client decrypts N_t and \tilde{x}_t
- Update $\alpha_t, \beta_t, \nu_t, m_t$

$$\alpha_t = \alpha_0 + N_t \quad (14)$$

$$\beta_t = \beta_0 + N_t \quad (15)$$

$$\nu_t = \nu_0 + N_t \quad (16)$$

$$m_t = \frac{1}{\beta_t} (\beta_0 m_0 + N_t \tilde{x}_t) \quad (17)$$

- Compute the covariance matrix S'_t of the local data which belongs to t -th mode

$$S'_t = \sum_{n=1}^{N_c} r_{nt} (x_n - \tilde{x}_t)(x_n - \tilde{x}_t)^T \quad (18)$$

- Send $HE(S'_t)$ to the server

Step 5 (Variational M step): Server

- Get $HE(S'_t)$ from each client
- Update the global covariance matrix S_t by S'_t from each client $c \in C$

$$HE(S_t) = \frac{1}{N_t} \sum_{c \in C} HE(S'_t) \quad (19)$$

- Send $HE(S_t)$ to each client

Step 6 (Convergence check): Client

- Each client decrypts S_t from the server
- Update the parameter W

$$W_t^{-1} = W_0^{-1} + \frac{\beta_0 N_t}{\beta_0 + N_t} (\bar{x}_t - m_0)(\bar{x}_t - m_0)^T + N_t S_t \quad (20)$$

- Update the lower bound L

$$\begin{aligned} L = & - \sum_{n=1}^{N_c} \sum_{t=1}^T (e^{r_{nt}} \times r_{nt}) \\ & - \sum_{t=1}^T \left(\frac{\nu_t D \ln 2}{2} - \sum_{t=1}^T \ln \Gamma(\nu_t) \right) \\ & - \left(\ln \Gamma \left(\sum_{t=1}^T \alpha_t \right) - \sum_{t=1}^T \ln \Gamma(\alpha_t) \right) \\ & - \frac{D \sum_{t=1}^T \ln \beta_t}{2} - \sum_{t=1}^T (\nu_t |W_t|) - \sum_{t=1}^T (\nu_t |W_t|) \end{aligned} \quad (21)$$

- Send L to the server

Step 7 (Convergence check): Server

- Get the lower bound L from the client in this iteration and compare it with the last L_{last} . If the difference between them is less than a predefined value ϵ , the process ends. Otherwise, return to the Step 2.

B Derivation of Global Mean and Covariance

We suppose that each client possesses a local tabular dataset $X_k = [x_{k,j}]^{N_k} \in \mathcal{R}^{N_k \times l}$, where $N_k > 1$ represents the number of samples of k -th client. The global dataset is $X = (X_1, X_2, \dots, X_K)$, where K indicates the number of clients. Then, the global mean is

$$\begin{aligned} E(X) &= \frac{1}{N} \sum_{k=1}^K \sum_{j=1}^{N_k} x_{k,j} = \sum_{k=1}^K \frac{N_k}{N} \cdot \frac{1}{N_k} \sum_{j=1}^{N_k} x_{k,j} \\ &= \sum_{k=1}^K \frac{N_k}{N} E(X_k) \end{aligned} \quad (22)$$

where $E(X) \in \mathcal{R}^{1 \times l}$. The global covariance is

$$\begin{aligned} \Sigma_X &= E[(X - E(X))^T (X - E(X))] \\ &= E(X^T X) - E^T(X)E(X) \end{aligned} \quad (23)$$

For $X^T X$, we have

$$\begin{aligned} X^T X &= [X_1^T, X_2^T, \dots, X_K^T] \begin{bmatrix} X_1 \\ X_2 \\ \vdots \\ X_K \end{bmatrix} \\ &= \sum_{k=1}^K X_k^T X_k = \sum_{j=1}^{N_k} x_{k,j}^T x_{k,j} \in \mathcal{R}^{l \times l} \end{aligned} \quad (24)$$

Then, we can compute $E(X^T X) = E(\sum_{k=1}^K X_k^T X_k) = \sum_{k=1}^K E(X_k^T X_k)$. Finally, the global covariance is

$$\begin{aligned} \Sigma_X &= E(X^T X) - E^T(X)E(X) \\ &= \sum_{k=1}^K E(X_k^T X_k) - E^T(X)E(X) \\ &= \sum_{k=1}^K E(X_k^T X_k) - \left(\sum_{k=1}^K \frac{N_k}{N} E(X_k) \right)^T \left(\sum_{k=1}^K \frac{N_k}{N} E(X_k) \right) \end{aligned} \quad (25)$$

From Equation (25), to obtain the global covariance, we need compute $E(X_k)$ and $E(X_k^T X_k)$ in each client.

C Proof of Theorem 1

Theorem 1. $X \sim N(0, I)$, $X \in \mathcal{R}^{N \times l}$, the covariance of X is Σ_X and its Cholesky decomposition is $\Sigma_X = UU^T$. For $\forall L \sim N(0, I)$, $L \in \mathcal{R}^{N \times l}$. $Y = LU^T \in \mathcal{R}^{N \times l}$, we have $\Sigma_X = \Sigma_Y$

Proof.

$$\begin{aligned} \Sigma_Y &= E[(Y - E(Y))^T (Y - E(Y))] \\ &= E[(Y^T - E(Y)^T)(Y - E(Y))] \\ &= E[Y^T Y - E(Y)^T Y - Y^T E(Y) + E(Y)^T E(Y)] \\ &= E[UL^T LU^T - UE(L)^T LU^T - UL^T E(L)U^T \\ &\quad + UE(L)^T E(L)U^T] \\ &= UE[L^T L - E(L)^T L - L^T E(L) + E(L)^T E(L)]U^T \\ &= U\Sigma_L U^T \end{aligned} \quad (26)$$

where Σ_L represents the covariance of L . Since that L follows an independent standard normal distribution. Thus $\Sigma_L = I$. Then, we have,

$$\Sigma_Y = U\Sigma_L U^T = UU^T = \Sigma_X \quad (27)$$

D Computation complexity and Communication Costs

Since Fed-TDA introduces MDT, ICDM, and privacy preserving data synthesis on the vanilla FL framework, additional computation and communication overhead are incurred. In this section, we only discuss the additional computation and communication costs introduced by Fed-TDA, compared to vanilla FL.

Computation complexity On the server-side, as shown in Algorithm 1, the additional computation including federated GMM for each continuous columns, the global frequency for each discrete columns, and global covariance Σ . The computation complexity of federated GMM on the server is $O(Kmtnc)$, the global frequency is $O(Knd)$, and the global covariance is $O(Kl^2)$, where $l = (2n_c + n_d)$. Thus, the total computation complexity of Fed-TDA on the server is $O(K(4n_c^2 + 4n_c n_d + n_d^2 + mtn_c + n_d))$. On each client, as shown in Algorithm 1 and 2, the additional computation includes local parameters for federated GMM, local

Dataset	Number of samples	Number of training sets	Number of test set	Number of continuous columns	Number of discrete columns	Number of classes
Clinical	299	209	90	7	5	2
Tuberculosis	1550	1340	310	18135	0	2
CovType	581012	406704	174308	10	44	7
Intrusion	29991	20000	9991	38	3	10
Body	13393	9373	4020	10	1	4

Table 6: Statistic of datasets.

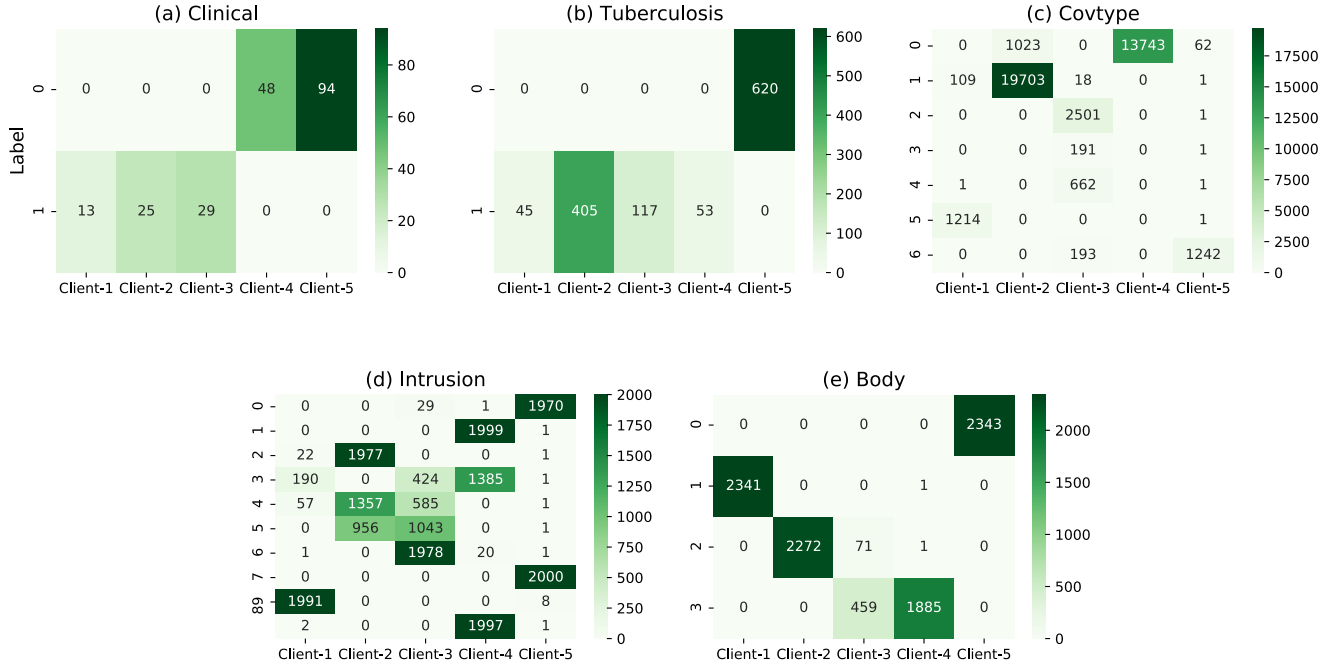


Figure 7: Label distributions of Clinical, Tuberculosis, CovType, Intrusion, and Body across the clients, where $\beta = 0.05$.

frequency for each discrete columns, DMT and ICDM for local data representation, local expectation for global covariance in Equation (25), and privacy preserving data synthesis. The computation complexity for the above process are $O(N_k m t n_c)$, $O(N_k n_d)$, $O(N_k l)$, $O(N_k l)$, and $O(N_k l)$, respectively. Therefore, the total additional computation complexity of each client is $O(N_k(6n_c + 4n_d + m t n_c))$.

Communication costs As shown in Figure 1, the exchanged statistics include the global covariance, federated VB-GMM, and ICDM. Specifically, for ICDM, each client uploads the local frequency for each category to the server and incurs $n_d p$ cost, where p represents the average number of categories for each discrete column. For federated VB-GMM, the communication cost of uploading is $(3t+2)n_c m$, where t represents the average number of Gaussian distributions for each continuous column and m is the number of learning rounds of federated VB-GMM. To compute global covariance, each client upload $E(X_k)$ and $E(X_k^T X_k)$ to the server, the cost is $l(l+1)$, where $l = 2n_c + n_d$. Thus, the total communication cost of uploading is $K(4n_c^2 + n_d^2 + 4n_c n_d + (3tm + 2m + 2)n_c + (p+1)n_d)$. For download, the

communication cost of ICDM is $n_d p$, the cost for federated VB-GMM is $(6t+1)n_c m$, and the cost of global covariance is l^2 . Then, the total communication cost of download is $K(4n_c^2 + n_d^2 + 4n_c n_d + n_d p + (6t+1)n_c m)$.

With the above analysis, we found that the additional computation and communication cost of Fed-TDA depends on the number of columns (e.g, n_c and n_d). In real-world applications, the number of table columns is much smaller than the number of samples, generally between tens to hundreds. Compared with the federated model training, the additional computation cost and communication overhead of Fed-TDA is almost negligible.

E Experimental Details

Datasets

We evaluate our Fed-TDA on five real-world datasets. Table 6 shows the statistics of datasets. The details of these datasets are as follows:

- **Clinical** (Chicco and Jurman 2020) is a dataset about Cardiovascular diseases (CVDs) that predicts mortality

from heart failure information, which contains 299 samples with 7 continuous columns and 5 discrete columns. This dataset is used for binary classification task.

- **Tuberculosis** (Warnat-Herresthal et al. 2021) is an RNA-seq dataset based on whole blood transcriptomes, which is used to predict tuberculosis from genetic information. This dataset contains 18135 continuous columns but 1550 samples, which is used for binary classification task.
- **CovType** (Blackard and Dean 1999) dataset is derived from US Geological Survey (USGS) and US Forest Service (USFS). The label attribute represents forest cover type, which contains seven classes. This dataset contains 581012 samples, where 406704 samples are training set and 174308 are used for testing. We found that the test performance of the model trained by taking 10% of the training set is close to the whole training data. To facilitate the experiment, we took 10% of the training set for the federated learning experiment.
- **Intrusion** is collected from the kddcup99 (Tavallae et al. 2009) dataset and contains the top 10 types of network intrusions. There are 20000 samples for training and 9991 samples for testing.
- **Body** (Kaggle 2022) dataset comes from Kaggle and is provided by Korea Sports Promotion Foundation for predicting body performance, which is used for multi-class classification task. This dataset contains 13393 samples with 10 continuous columns and 1 discrete columns, in which 9373 samples are used for training and other 4020 samples are used for testing.

Figure 7 shows the distributions of the above five datasets among the clients. From Figure 7, we can find that the label distributions are quite heterogeneous. In particular, the number of samples varies among the clients, and each client contains only a few classes of labels.

Implementation Details

Table 7 shows the details of our simple deep learning model used for classifier. Note that, the goal of our experiment is not to find an optimal classifier. Thus, this vanilla classifier is used for all experiments in this paper. Table 8 shows the detailed hyperparameters used in our experiments.

F Extra Experimental Results

Varying local epochs

Figure 8 investigates the impact of the number of local epochs on test performance, which shows the average test ROCAUC or accuracy of baseline methods on the Tuberculosis, CovType, and Body datasets. As the number of local epochs increases from 1 to 10, Fed-TDA achieves the best and most robust performance. The experimental results in these datasets are consistent with the other two datasets.

Privacy study

Figure 9 demonstrates the trade-off between the test performance of Fed-TDA and the privacy level on the Tuberculo-

Layer	Details
Input Layer	Linear(n_{input} , 512) BatchNorm1d(512) ReLU() Dropout()
Hidden Layer-1	Linear(512, 256) BatchNorm1d(256) ReLU() Dropout()
Hidden Layer-2	Linear(256, 128) BatchNorm1d(128) ReLU() Dropout()
Hidden Layer-3	Linear(128, 64) BatchNorm1d(64) ReLU() Dropout()
Output Layer	Linear(64, n_{output})

Table 7: Detailed information of our simple deep learning model. n_{input} represents the dimensional of input data and n_{output} represents the output dimension.

Hyperparameters	Details
Communication rounds	100
Optimizer	Adam
Learning rate	0.001
Weight decay	1e-5
Local epoch	3
Batch size	64
Dropout	5
Clients per round	5
μ for FedProx	0.05
M_k for Fedmix	5
λ for FedProx	0.05

Table 8: Hyperparameters used in our experiments.

sis, Clinical, and Body datasets. The test performance of our Fed-TDA improves as ϵ varies from 1 to ∞ .

Statistical Similarity

Table 9 shows the statistical similarity results of two GAN-based methods on Tuberculosis, CovType, and Body datasets. Since there is only one discrete column in Tuberculosis tables, we compute its average WD. We can find that our Fed-TDA consistently achieves the best similarity scores.

Visualisation of Synthesized Samples

We show some synthesized samples in Table 11, based on the Clinical dataset, which generated by our Fed-TDA. Some records of the origin Clinical dataset from three clients are shown in Table 10 after choosing a subset of columns for space consideration. In Table 10, rows 1-2 are from Client-1, rows 3-4 from Client-2, and the last two rows are from Client-3. As we can find, there is no one-to-one relationship between Table 10 and Table 11, and the real records have

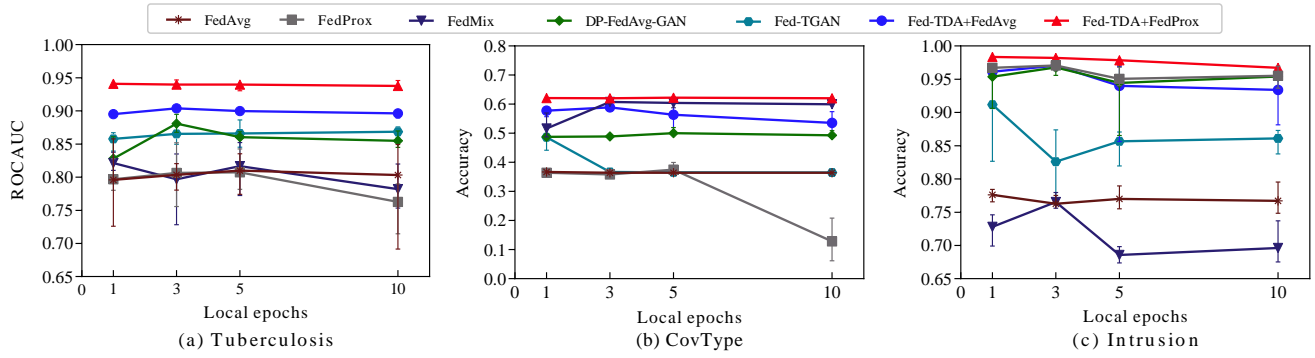


Figure 8: Test performance under varying number of local epochs on the Tuberculosis, CovType, and Body datasets. Where $\beta = 0.05$ and $K = 5$.

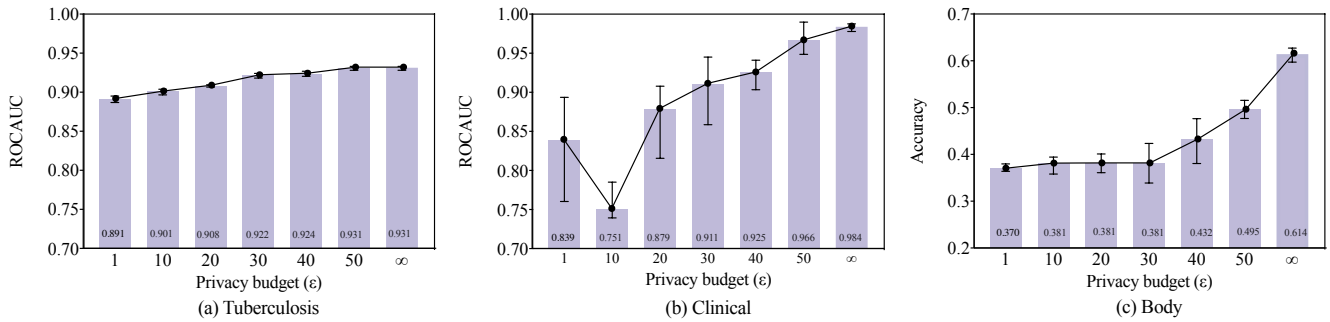


Figure 9: Trade-off between the test performance and the privacy level on the Tuberculosis, Clinical, and Body datasets. Where $\beta = 0.05$, $K = 5$, the local epoch is 3, privacy budget $\delta = 10^{-4}$ and ϵ varies from 1 to ∞ .

very different values from the synthesized record. It is almost impossible to re-identify the original information from the synthesized data.

Methods	Tuberculosis			CovType						Body					
	$\beta = 0.05$	$\beta = 0.1$	$\beta = 0.5$	$\beta = 0.01$		$\beta = 0.05$		$\beta = 0.1$		$\beta = 0.01$		$\beta = 0.05$		$\beta = 0.1$	
	WD	WD	WD	JSD	WD	JSD	WD	JSD	WD	JSD	WD	JSD	WD	JSD	WD
DP-FedAvg-GAN	0.179	0.192	0.201	0.374	0.429	0.333	0.353	0.397	0.260	0.134	0.315	0.150	0.371	0.230	0.319
Fed-TGAN	0.178	0.201	0.205	0.100	0.085	0.099	0.103	0.110	0.102	0.077	0.080	0.067	0.075	0.037	0.076
Fed-TDA	0.141	0.132	0.145	0.102	0.099	0.102	0.099	0.102	0.099	0.066	0.068	0.066	0.068	0.066	0.068

Table 9: The statistical similarity for DP-FedAvg-GAN, Fed-TGAN, and Fed-TDA. Where $K = 5$.

	age	anaemia	phosphokinase	platelets	sex	smoking	time	label
1	73	0	582	203000	1	0	195	0
2	75	1	246	127000	1	0	10	1
3	50	0	369	252000	1	0	90	0
4	57	1	129	395000	0	0	42	1
5	55	0	109	254000	1	1	60	0
6	45	0	582	166000	1	0	14	1

Table 10: Sample records in the origin Clinical table of each client.

	age	anaemia	phosphokinase	platelets	sex	smoking	time	label
1	51	0	2120	313120	1	1	209	0
2	51	0	1425	216723	0	1	66	1
3	59	1	470	272237	0	0	77	0
4	72	1	23	264638	1	0	59	1
5	74	1	309	298268	0	1	55	0
6	56	1	23	368381	1	0	6	1

Table 11: Sample records in the synthesized Clinical table by Fed-TDA.